Numerical Pricing of Coupon Bonds and Derivatives in a Stochastic Interest Rate Environment Using Crank-Nicolson

Abhishek Ranjan Dey

1 Coupon Bonds with a Stochastic Interest Rate

1.1 Introduction and problem formulation

The task begins with a coupon bond whose price is denoted by $B(r,t;T)$, where the short rate r follows a risk-neutral stochastic process:

$$dr = \kappa(\theta e^{\mu t} - r)dt + \sigma r^{\beta} dW_t. \tag{1}$$

For market fit parameters $\mu = 0.0141, \kappa = 0.09389, \theta = 0.0289, \sigma = 0.116, \beta = 0.418$. The bond pays coupons continuously at $Ce^{-\alpha t}$, where $C = 10.2, \alpha = 0.01$. As the problem takes place under the risk-neutral measure $\mathbb{Q}$, and the coupons count as a continuous cash flow, the bond can only pay at the risk-free rate, minus the cash flow from the coupons:

$$dB = (rB - Ce^{-\alpha t})dt + (f(B,r,t))dW_t. \tag{2}$$

Where $f(B,r,t) = \sigma r^{\beta}\frac{\partial B}{\partial r}$ is the diffusion term, which arises through Itô's lemma. By applying Itô's lemma to the bond, and grouping dt terms, the above bond can be rewritten in terms of a PDE for the bond price $B(r,t;T)$:

$$\frac{\partial B}{\partial t} + \kappa(\theta e^{\mu t} - r)\frac{\partial B}{\partial r} + \frac{1}{2}\sigma^2 r^{2\beta}\frac{\partial^2 B}{\partial r^2} - rB + Ce^{-\alpha t} = 0. \tag{3}$$

This partial differential equation (PDE) is then subject to the boundary conditions:

$$B(r,T;T) = F, \tag{4}$$

$$\frac{\partial B}{\partial t} + \kappa\theta e^{\mu t}\frac{\partial B}{\partial r} + Ce^{-\alpha t} = 0 \quad \text{at } r = 0, \tag{5}$$

$$B(r,t;T) \to 0 \quad \text{as } r \to \infty. \tag{6}$$

The PDE is defined on $r \in [0,\infty]$ and $t \in [0,T]$, for the bond expiry $T = 3$, and face value $F = 240$. This document discusses the solution to this PDE with the appropriate boundary conditions using a Crank-Nicolson (CN) finite difference scheme. The CN scheme operates by discretising the (r,t) domain into a grid, and approximating the evolution of the bond price $B(r,t;T)$ at each grid point. The scheme achieves second-order accuracy in space and time, with an error of $O(\Delta r^2, \Delta t^2)$.

The time interval $[0,T]$ is discredited into $i_{\max}$ steps with uniform spacing $\Delta t = \frac{T}{i_{\max}}$. Therefore, the set of grid points in time is described by $i \in \mathbb{N}[0, i_{\max}]$, and a time step is described as $t_i = i\Delta t$. Similarly, the $r \in [0,\infty]$ is discretised by introducing an arbitrarily large $r_{\max}$ to truncate this domain, and discretising $r \in [0, r_{\max}]$ with steps $\Delta r = \frac{r_{\max}}{j_{\max}}$, and as such each step in r can be described as $r_j = j\Delta r$, for $j \in \mathbb{N}[0, j_{\max}]$.

At each time step, the Crank-Nicolson (CN) method computes the solution by averaging the discretised values of the bond price B and its spatial derivatives between time levels i and $i+1$. This approach effectively evaluates the bond at the intermediate time $t = (i + \frac{1}{2})\Delta t$, which is what grants the scheme second-order accuracy in time $O(\Delta t^2)$.

Second-order accuracy in space $O(\Delta r^2)$ is achieved by applying a centred difference scheme for spatial derivatives, where the value at each grid point j depends on its immediate neighbours $j-1$ and $j+1$.

At each time step, this discretisation leads to a tridiagonal linear system of the form

$$a_j B^i_{j-1} + b_j B^i_j + c_j B^i_{j+1} = d_j, \tag{7}$$

where a_j, b_j, and c_j are the coefficients arising from the discretisation of the PDE, d_j depends on known values from the previous time step $i+1$, and $B^i_j = B(r_j, t_i)$.

1.2 Discretisation of bond PDE and boundary conditions

The Crank-Nicolson scheme for Eq.(3) is written using the definitions below:

$$B(r_j, t_{i+1/2}) \approx \frac{1}{2}(B_j^i + B_j^{i+1}) \tag{8a}$$

$$\frac{\partial B}{\partial t} \approx \frac{1}{\Delta t}\left(B_j^{i+1} - B_j^i\right) \tag{8b}$$

$$\frac{\partial B}{\partial r} \approx \frac{1}{4\Delta r}\left(B_{j+1}^{i+1} - B_{j-1}^{i+1} + B_{j+1}^i - B_{j-1}^i\right) \tag{8c}$$

$$\frac{\partial^2 B}{\partial r^2} \approx \frac{1}{2\Delta r^2}\left(B_{j+1}^{i+1} - 2B_j^{i+1} + B_{j-1}^{i+1} + B_{j+1}^i - 2B_j^i + B_{j-1}^i\right) \tag{8d}$$

This leads to the coefficients in Eq.(7) being:

$$a_j = \frac{\sigma^2 (j\Delta r)^{2\beta}}{4(\Delta r)^2} - \frac{\kappa(\theta e^{\mu(i+\frac{1}{2})\Delta t} - j\Delta r)}{4\Delta r}, \tag{9a}$$

$$b_j = -\frac{1}{\Delta t} - \frac{1}{2} j\Delta r - \frac{\sigma^2 (j\Delta r)^{2\beta}}{2(\Delta r)^2}, \tag{9b}$$

$$c_j = \frac{\sigma^2 (j\Delta r)^{2\beta}}{4(\Delta r)^2} + \frac{\kappa(\theta e^{\mu(i+\frac{1}{2})\Delta t} - j\Delta r)}{4\Delta r}, \tag{9c}$$

$$\begin{aligned} d_j = &-B_{j-1}^{i+1}\left[\frac{\sigma^2 (j\Delta r)^{2\beta}}{4(\Delta r)^2} - \frac{\kappa(\theta e^{\mu(i+\frac{1}{2})\Delta t} - j\Delta r)}{4\Delta r}\right] - B_j^{i+1}\left[\frac{1}{\Delta t} - \frac{1}{2} j\Delta r - \frac{\sigma^2 (j\Delta r)^{2\beta}}{2(\Delta r)^2}\right] \\ &- B_{j+1}^{i+1}\left[\frac{\sigma^2 (j\Delta r)^{2\beta}}{4(\Delta r)^2} + \frac{\kappa(\theta e^{\mu(i+\frac{1}{2})\Delta t} - j\Delta r)}{4\Delta r}\right] - Ce^{-\alpha(i+\frac{1}{2})\Delta t}. \end{aligned} \tag{9d}$$

The boundary condition in Eq.(5) is discretised with the same definition as the PDE discretisation, however, the spatial r derivative is handled with a three-point method:

$$\frac{\partial B}{\partial r} \approx \frac{1}{4\Delta r}\left[4B_{j+1}^i - B_{j+2}^i - 3B_j^i + 4B_{j+1}^{i+1} - B_{j+2}^{i+1} - 3B_j^{i+1}\right]. \tag{10}$$

Through this discretisation, the LHS boundary condition ends up with a non-tridiagonal setup. It is incompatible with the CN method, and as such this dependency is removed by considering the 1st j, which must satisfy Eqs.(9). This gives two equations that must hold at the same time, and as such leads to the ability to define $\tilde{a}_0, \tilde{b}_0, \tilde{c}_0, \tilde{d}_0$ that hold at $t = 0$, and conform to the tridiagonal formulation. By direct substitution of Eq.(10), the coefficients returned satisfy $a_0 B_0^i + b_0 B_1^i + c_0 B_2^i = d_j$, with coefficients:

$$a_0 = -\frac{1}{\Delta t} - \frac{3\kappa\theta e^{\mu(i+\frac{1}{2})\Delta t}}{4\Delta r}, \tag{11a}$$

$$b_0 = \frac{\kappa\theta e^{\mu(i+\frac{1}{2})\Delta t}}{\Delta r}, \tag{11b}$$

$$c_0 = -\frac{\kappa\theta e^{\mu(i+\frac{1}{2})\Delta t}}{4\Delta r}, \tag{11c}$$

$$d_0 = -B_0^{i+1}\left[\frac{1}{\Delta t} - \frac{3\kappa\theta e^{\mu(i+\frac{1}{2})\Delta t}}{4\Delta r}\right] - B_1^{i+1}\left[\frac{\kappa\theta e^{\mu(i+\frac{1}{2})\Delta t}}{\Delta r}\right] - B_2^{i+1}\left[\frac{\kappa\theta e^{\mu(i+\frac{1}{2})\Delta t}}{4\Delta r}\right] - Ce^{\alpha(i+\frac{1}{2})\Delta t} \tag{11d}$$

Finally, the modified coefficients, which preserve the tridiagonal structure and maintain compatibility with the CN discretisation, satisfy the relation $\tilde{b}_0 B_0^i + \tilde{c}_0 B_1^i = d_0$, are given by:

$$\tilde{a}_0 = 0, \tag{12a}$$

$$\tilde{b}_0 = a_0 - \frac{c_0}{c_1} a_1, \tag{12b}$$

$$\tilde{c}_0 = b_0 - \frac{c_0}{c_1} b_1, \tag{12c}$$

$$\tilde{d}_0 = d_0 - \frac{c_0}{c_1} d_1. \tag{12d}$$

The coefficients using gridpoint $j = 1$ utilise the definition as in Eq.(8)(a). These coefficients are the coefficients used at the boundary and passed through the tridiagonal solver. The boundary condition Eq.(6) is satisfied simply through substitution, and leads to the upper boundary coefficients satisfying:

$$a_{j_{\max}} = c_{j_{\max}} = 0, \tag{13a}$$

$$b_{j_{\max}} = 1, \tag{13b}$$

$$d_{j_{\max}} = -B_{j_{\max}}^{i+1} \tag{13c}$$

1.3 Computation of bond value with limited grid points

The value of the bond at $r = r_0 = 0.0238$ and at time $t = 0$ with $i_{\max} = j_{\max} = 100$, and $r_{\max} = 1.0$ is:

$$B(r_0, t = 0; T) = 254.8497836346682. \tag{14}$$

The linear system is solved with LU decomposition, and this value is found from the nearest grid point, $r_j = 0.02$, as the exact value can only be calculated. This estimate can be improved by using Scipy's `RegularGridInterpolator`, which can take the bond solution surface B_j^i, and interpolates between known values by linearly combining nearby gridpoints, effectively smoothing the solution, and allowing for evaluation at $r_0 = 0.0238$ without introducing more grid points. This yields the value:

$$B(r_0, t = 0; T) = 252.5483669793577. \tag{15}$$

Which is the best estimate of the bond at $r = r_0$ and $t = 0$, with $i_{\max} = j_{\max} = 100$ and an $r_{\max} = 1.0$.

1.4 The effect of an alternate boundary condition

The values in section 1.3 used the RHS boundary in Eq.(6), called the Dirichlet boundary condition, which enforces the bond is valueless at very high interest rates. The Neumann boundary condition is more forgiving and assumes the bond price smoothly flattens out as $r \to \infty$. This boundary condition is given by:

$$\frac{\partial B}{\partial r} \to 0 \quad \text{as } r \to \infty. \tag{16}$$

This boundary condition is handled with the backwards three-point difference formula:

$$\frac{1}{4\Delta r}[B_{j_{\max}-2}^i - 4B_{j_{\max}-1}^i + 3B_{j_{\max}}^i + B_{j_{\max}-2}^{i+1} - 4B_{j_{\max}-1}^{i+1} + 3B_{j_{\max}}^{i+1}] \tag{17}$$

As in the case of the forward three-point method, this allows for an $O(\Delta r^2, \Delta t^2)$ handling of the $r_{\max}$ boundary, maintaining the CN accuracy. This method again requires the use of simultaneous equations, one that comes from direct substitution of Eq.(17) into Eq.(16), and another that comes from Eqs.(9) at $j = j_{\max} - 1$. This leads to:

$$a_{j_{\max}} = 1, \tag{18a}$$

$$b_{j_{\max}} = -4, \tag{18b}$$

$$c_{j_{\max}} = 3, \tag{18c}$$

$$d_{j_{\max}} = -B_{j_{\max}-2}^{i+1} + 4B_{j_{\max}-1}^{i+1} - 3B_{j_{\max}}^{i+1} \tag{18d}$$

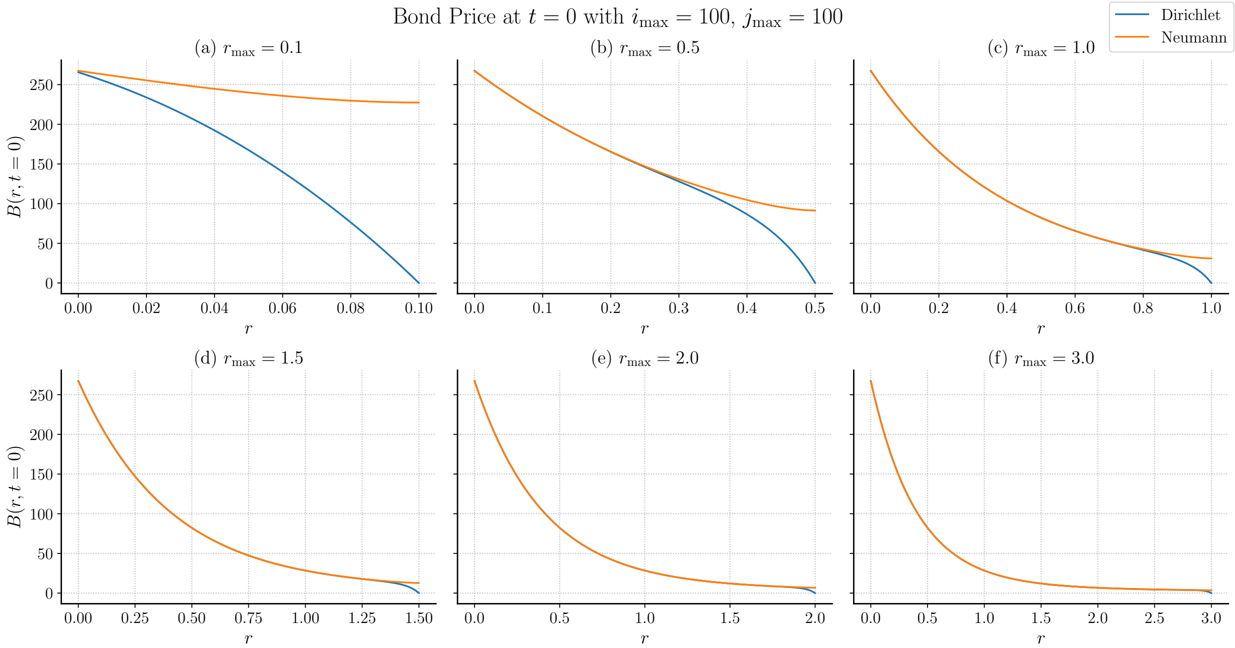

Figure 1: The effect of $r_{\max}$ on the value of the bond $B(r, t; T)$ at $t = 0$.

.

Through the same elimination process, the coefficients of the tridiagonal system at the RHS boundary:

$$\tilde{a}_{j_{\max}} = b_{j_{\max}} - \frac{a_{j_{\max}}}{a_{j_{\max}-1}} b_{j_{\max}-1}, \tag{19a}$$

$$\tilde{b}_{j_{\max}} = c_{j_{\max}} - \frac{a_{j_{\max}}}{a_{j_{\max}-1}} c_{j_{\max}-1}, \tag{19b}$$

$$\tilde{c}_{j_{\max}} = 0, \tag{19c}$$

$$\tilde{d}_{j_{\max}} = d_{j_{\max}} - \frac{a_{j_{\max}}}{a_{j_{\max}-1}} d_{j_{\max}-1}. \tag{19d}$$

Figure 1 displays how each of the boundaries, Dirichlet (Eq.(5)), and Neumann (Eq.(16)) vary with $r_{\max}$. All plots show the value of the bond at $t = 0$, and at low $r_{\max}$. Varying $r_{\max}$ can have a significant effect, as the implemented solution can only work on a truncated spatial domain where it should hold that $[0, r_{\max}] \approx [0, \infty]$ in an applied case. It is therefore natural that the treatment of this truncation and its value will drastically alter the solution.

The Dirichlet condition assumes the bond price has already decayed to zero at the boundary. Imposing this condition is a hard constraint, and means the numerical solution is always forced to zero at $r = r_{\max}$, which may cause an artificial steepening near the boundary, which can also affect the PDE solution in the interior. The Neumann boundary condition does not fix the value of B and instead flattens the boundary, meaning there are no gradients as $r \to \infty$. Financially, this means that as interest rates increase, the bond value decreases slowly. In this way, the Neumann condition can be seen as letting the solution naturally settle.

This is reflected in Figure 1, which displays the dependency of each boundary condition on the truncation value $r_{\max}$. At $r \leq 1$ (Figure 1(a-c)), there is a pronounced difference between the two boundary conditions. The Dirichlet curves down as r approaches $r_{\max}$, whilst the Neumann condition permits a more gradual decrease, which is consistent with the behaviour that is seen in both solutions by increasing $r_{\max}$. Once the $r_{\max}$ is increased far enough beyond the economically relevant range, the strong effect of the Dirichlet

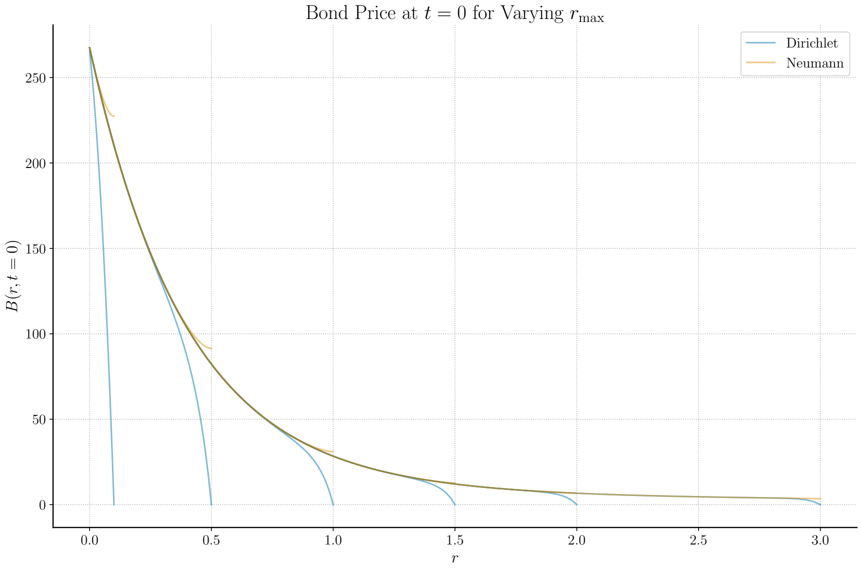

Figure 2: Each of the solutions in Figure 1 in one plot, displaying how each scheme diverges for different $r_{\max}$.

boundary reduces in size, and the results within the range of economically relevant rates are identical, with a sharp decrease at $r_{\max}$.

The Neumann boundary condition smoothing at $r_{\max}$ can be seen in Figure 2, the gradient of the solution decreases as each boundary is approached. The figure also frames how, at low $r_{\max}$, the Dirichlet boundary condition can lead to solutions that are not consistent, an example of how Dirichlet can enforce errors that are global on the truncated domain. In contrast, the errors enforced by the Neumann boundary are localised to $r \approx r_{\max}$. This leads to the conclusion that for a truncated domain, the Neumann boundary condition $\frac{\partial B}{\partial r} \to 0$ is more suitable and produces more consistent results that are less sensitive to $r_{\max}$.

1.5 Accurate computation of the bond value

To accurately compute the value of the bond at $t = 0$, and $r_0 = 0.0238$, the values of Δt, Δr must be considered. As section 1.2 indicates, the value of $r_{\max}$ may also affect the value of $B(r_0, t = 0; T)$, and so a sufficiently large $r_{\max}$ must be considered, along with a $j_{\max}$ that allow for r_0 to appear as a point on the grid. A suitably high $r_{\max} = 4.0$ is used, which requires a $j_{\max} = 20,000$.

Figure 3 shows that the discrepancy with varying $i_{\max}$ is very small $O(10^{-6})$, even at very high values, for this reason, $i_{\max} = 2200$ is used, as this is the value for which the discrepancy reaches below 5×10^{-6}, the point at which it converges. Using these parameters, $r_0 = 0.0238$, $i_{\max} = 2200$,$j_{\max} = 20,000$,$r_{\max} = 4.0$, Neumann boundary at $r_{\max}$, and all the parameters outlined in section 1.1. This gives $B(r_0, t = 0; T)$:

$$B(r_0, t = 0; T) = 252.5327633044924 \tag{20}$$

2 American put option on a bond

2.1 Introduction and problem formulation

The next task considers an option V to buy the bond at time $T_1 = 1.02$. Let $V(r, t; T_1, T)$ be the value of the put option to sell the coupon bond $B(r, t, T)$ at time T_1, where the option matures at time T. Again, by considering that the option can only evolve at the risk-free rate $rV dt$, Itô's lemma can be utilised to return

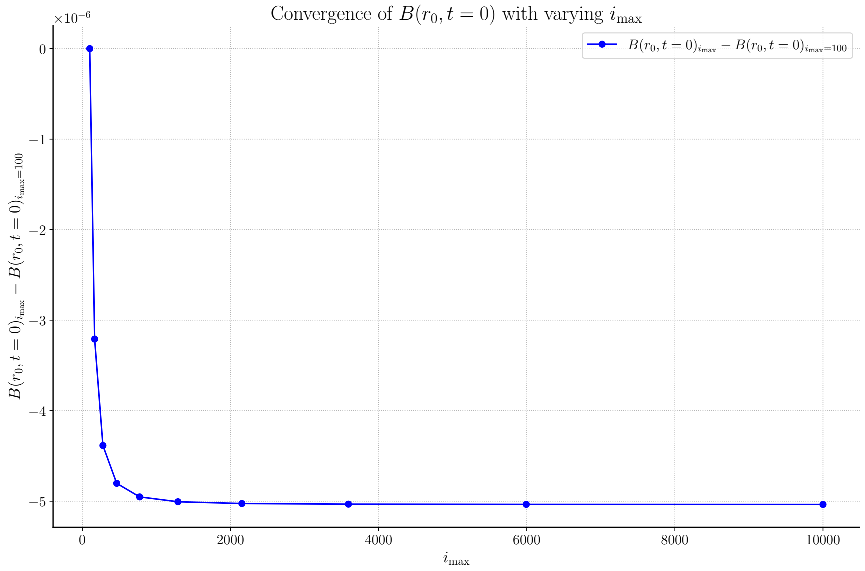

Figure 3: The dependence of $B(r_0, t = 0; T)$ on the value of $i_{\max}$.

a PDE that the option must satisfy.

$$\frac{\partial V}{\partial t} + \kappa(\theta e^{\mu t} - r)\frac{\partial V}{\partial r} + \frac{1}{2}\sigma^2 r^{2\beta}\frac{\partial^2 V}{\partial r^2} - rV = 0. \tag{21}$$

The put option pays at expiry:

$$V(r, t = T_1; T_1, T) = \max(X - B(r, T_1; T), 0). \tag{22}$$

The option must also have the option to exercise early, with a strike price $X = 245$:

$$V(r, t; T_1, T) = X - B(r, t; T). \tag{23}$$

Therefore, by no arbitrage arguments, and due to the early exercise condition, the option must satisfy the early exercise condition for $t \leq T_1$:

$$V(r, t; T_1, T) \geq \max(X - B(r, t; T), 0). \tag{24}$$

The PDE itself is subject to boundary conditions

$$\frac{\partial V}{\partial t} + \kappa\theta e^{\mu t}\frac{\partial V}{\partial r} = 0 \quad \text{at } r = 0, \tag{25}$$

$$V(r, t; T_1, T) \to X - B(r, t; T) \quad \text{as } r \to \infty. \tag{26}$$

The CN grid is set up identically to that of the coupon bond, with the domain defined as $t \in [0, T]$ and $r \in [0, r_{\max}]$. However, the option PDE is only solved for $t \leq T_1 < T$. The reason for constructing the full-time grid up to T is to allow for exact reuse of gridpoints from the bond price surface B when evaluating the American option. In particular, since $T_1 = 1.02$, choosing any multiple of $i_{\max} = 100$ ensures that T_1 aligns exactly with a discrete time node. This allows the precomputed bond surface to be directly reused in evaluating the early exercise condition and expiry payoff in Eqs.(22), (23), and (26).

2.2 discretisation of option PDE and boundary conditions.

The PDE is discretised to CN $O(\Delta t^2, \Delta r^2)$, adhering to the definitions of V and its derivatives, identically to those in Eqs.(8), evaluating the bond at $(i+\frac{1}{2})\Delta t$ at each gridpoint. This leads to a set-up as in Eq.(7) again, with coefficients:

$$a_j = \frac{\sigma^2 (j\Delta r)^{2\beta}}{4(\Delta r)^2} - \frac{\kappa(\theta e^{\mu i \Delta t} - j\Delta r)}{4\Delta r}, \tag{27a}$$

$$b_j = -\frac{1}{\Delta t} - \frac{\sigma^2 (j\Delta r)^{2\beta}}{2(\Delta r)^2} - \frac{1}{2} j\Delta r, \tag{27b}$$

$$c_j = \frac{\sigma^2 (j\Delta r)^{2\beta}}{4(\Delta r)^2} + \frac{\kappa(\theta e^{\mu i \Delta t} - j\Delta r)}{4\Delta r}, \tag{27c}$$

$$\begin{aligned} d_j = &-V_{j-1}^{i+1}\left[\frac{\sigma^2 (j\Delta r)^{2\beta}}{4(\Delta r)^2} - \frac{\kappa(\theta e^{\mu i \Delta t} - j\Delta r)}{4\Delta r}\right] \\ &-V_j^{i+1}\left[\frac{1}{\Delta t} - \frac{\sigma^2 (j\Delta r)^{2\beta}}{2(\Delta r)^2} - \frac{1}{2} j\Delta r\right] \\ &-V_{j+1}^{i+1}\left[\frac{\sigma^2 (j\Delta r)^{2\beta}}{4(\Delta r)^2} + \frac{\kappa(\theta e^{\mu i \Delta t} - j\Delta r)}{4\Delta r}\right]. \end{aligned} \tag{27d}$$

The boundary condition Eq.(25) holds at $j = 0$, again a 3-point forward difference is used to maintain the Crank-Nicolson $O(\Delta r^2)$ accuracy at the boundary, as in Eq.(10). This results in the same elimination method, using Eqs.(27) to get a_1, b_1, c_1, d_1, and resulting in:

$$a_0 = -\frac{1}{\Delta t} - \frac{3\kappa\theta e^{\mu(i+\frac{1}{2})\Delta t}}{4\Delta r}, \tag{28a}$$

$$b_0 = \frac{\kappa\theta e^{\mu(i+\frac{1}{2})\Delta t}}{\Delta r}, \tag{28b}$$

$$c_0 = -\frac{\kappa\theta e^{\mu(i+\frac{1}{2})\Delta t}}{4\Delta r}, \tag{28c}$$

$$d_0 = -V_0^{i+1}\left[\frac{1}{\Delta t} - \frac{3\kappa\theta e^{\mu(i+\frac{1}{2})\Delta t}}{4\Delta r}\right] - V_1^{i+1}\left[\frac{\kappa\theta e^{\mu(i+\frac{1}{2})\Delta t}}{\Delta r}\right] - V_2^{i+1}\left[-\frac{\kappa\theta e^{\mu(i+\frac{1}{2})\Delta t}}{4\Delta r}\right]. \tag{28d}$$

Through the same elimination method as in section 1, the final coefficients to pass into the tridiagonal system:

$$\tilde{a}_0 = 0, \tag{29a}$$

$$\tilde{b}_0 = a_0 - \frac{c_0}{c_1} a_1, \tag{29b}$$

$$\tilde{c}_0 = b_0 - \frac{c_0}{c_1} b_1, \tag{29c}$$

$$\tilde{d}_0 = d_0 - \frac{c_0}{c_1} d_1. \tag{29d}$$

The r_{max} boundary in Eq.(26) is discretised using the time centered approach in Eq.(8a), and holds at j_{max}, resulting in:

$$a_{j_{\text{max}}} = c_{j_{\text{max}}} = 0, \tag{30a}$$

$$b_{j_{\text{max}}} = \frac{1}{2}, \tag{30b}$$

$$d_{j_{\text{max}}} = X - B_{j_{\text{max}}}^i - \frac{1}{2} V_{j_{\text{max}}}^{i+1}. \tag{30c}$$

2.3 Early exercise handling: PSOR

For European options, the Crank-Nicolson method leads to a linear system of the form $\mathbf{A}\vec{V}^i = \vec{d}$. At each time step i, this can be solved using an efficient LU solver, as in section 1, due to $\mathbf{A}$ having a tridiagonal form. However, in the case of an American option, the possibility of early exercise introduces an inequality constraint on the solution; every timestep must satisfy Eq.(24).

The American option must satisfy this constraint, as well as the PDE, at every point in the domain. Standard solvers cannot guarantee that this inequality will hold, which is why Projected Successive Over-Relaxation (PSOR) is used. At each time step, PSOR solves the Crank–Nicolson scheme by iterating over the spatial domain and updating each node using the most recent available values. For a given PSOR iteration k, the method estimates an intermediate value:

$$y_j^{i,k+1} = \frac{1}{b_j}\left(d_j^i - a_j V_{j-1}^{i,k+1} - c_j V_{j+1}^{i,k}\right), \tag{31}$$

using the coefficients from Eq.(7). The value is then relaxed using an over-relaxation factor $\omega \in [1,2]$, taken to be $\omega = 1.2$:

$$\tilde{V}_j^{i,k+1} = V_j^{i,k} + \omega\left(y_j^{i,k+1} - V_j^{i,k}\right). \tag{32}$$

To enforce the early exercise condition, this value is projected:

$$V_j^{i,k+1} = \max\left(\tilde{V}_j^{i,k+1},\ X - B_j^i\right). \tag{33}$$

This iteration proceeds until the squared update difference across all grid points satisfies

$$\sum_j \left(V_j^{i,k+1} - V_j^{i,k}\right)^2 \leq \varepsilon^2, \tag{34}$$

where $\varepsilon = 10^{-8}$. Boundary points are handled separately by omitting unavailable terms. The result is a stable and convergent scheme that respects both the structure of the Crank-Nicolson discretisation and the early exercise feature inherent to American options.

2.4 American option value

The option is initially solved over a square grid with resolution $i_{\max} = j_{\max} = 1000$. This relatively coarse grid is intentionally chosen to investigate the qualitative behaviour of the American option's early exercise boundary under varying values of $r_{\max}$, the upper bound of the interest rate domain. Figure 4 illustrates the option's payoff at times $t = 0$ and $t = T_1$ for $r_{\max} = 1.0$, highlighting the location of the early exercise boundary.

For this configuration, the estimated threshold interest rate at which early exercise becomes optimal is:

$$r_{\text{exercise}} = 0.032. \tag{35}$$

Although this value could be refined by increasing $j_{\max}$ (i.e., by improving spatial resolution), the coarse grid already captures the key qualitative feature: the relative flatness of the early exercise boundary across time, as visible in Figure 4.

Table 1 presents the early exercise threshold for a range of $r_{\max}$ values. These results suggest that the location of the exercise boundary is largely insensitive to the choice of $r_{\max}$ within the examined range. This behaviour is expected, as the early exercise region lies within the domain's interior. Consequently, the boundary condition imposed at $r = r_{\max}$ has negligible influence on the computed exercise threshold. A similar insensitivity to $r_{\max}$ is observed in the bond problem when using Neumann boundary conditions; as shown in Figure 1, the bond price solution remains largely unchanged for $r \ll r_{\max}$, reinforcing the idea that boundary effects at large r do not significantly affect the solution in the region of interest.

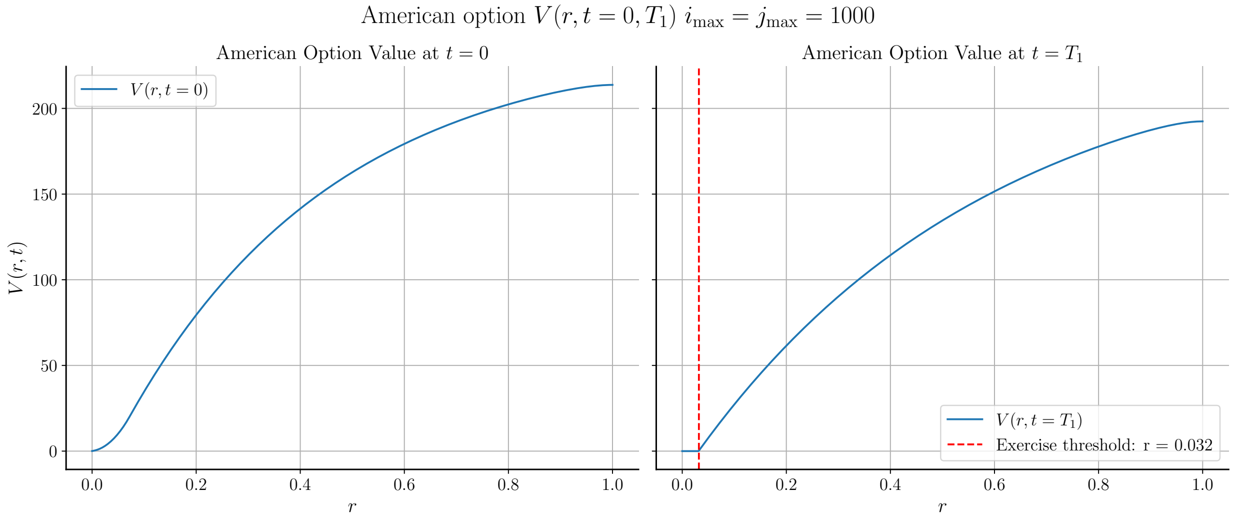

Figure 4: The exercise boundary for $i_{\max} = j_{\max} = 1000$ at $r_{\max} = 1.0$.

$r_{\max}$	1.00	1.50	2.00	2.50	3.00	3.50	4.00
r_{exercise}	0.0320	0.0315	0.0320	0.0325	0.0330	0.0315	0.0320

Table 1: Exercise threshold at $t = T_1$ vs domain boundary $r_{\max}$, $i_{\max} = j_{\max} = 1000$.

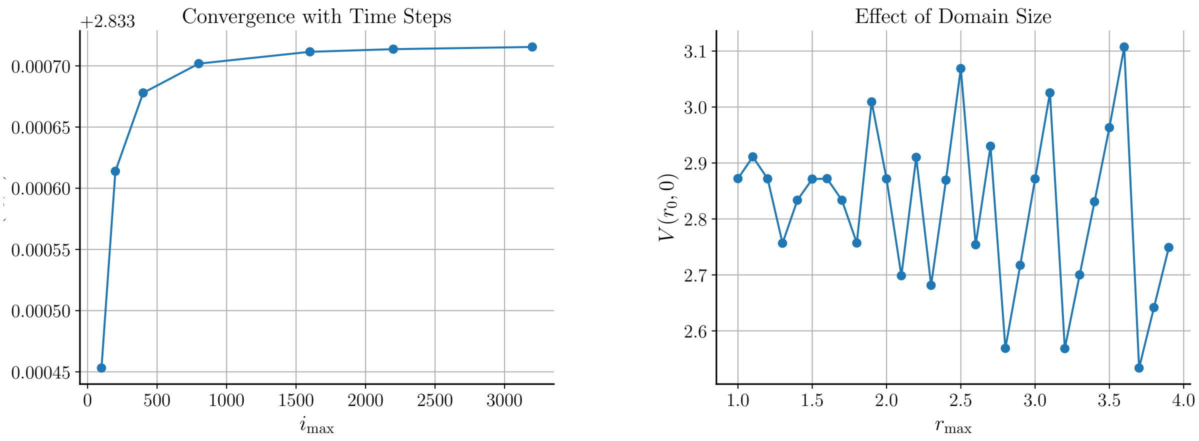

(a) $j_{\max} = 20000$, $r_{\max} = 4.0$

(b) $j_{\max} = i_{\max} = 1000$

Figure 5: Plots showing convergence behaviour of $V(r_0, t = 0)$ with varying $i_{\max}$ and $r_{\max}$.

Selecting $r_{\max} = 4$, in line with the best estimate used for the bond problem, necessitates setting $j_{\max} =$ 20,000 to maintain sufficient spatial resolution. The dependencies of the option value $V(r_0, t = 0)$ on both $i_{\max}$ and $r_{\max}$ are illustrated in Figure 5. In particular, Figure 5(b) demonstrates the solution's insensitivity to the choice of $r_{\max}$. Much like the exercise threshold, r_0 lies close to the lower boundary of the domain, and therefore does not feel the effects of the truncation at $r = r_{\max}$. The lack of an apparent trend with varying $r_{\max}$ suggests that observed errors are likely due to the absence of a grid point located exactly at

r_0, rather than from any boundary condition artefacts.

In contrast, the dependency on $i_{\max}$ reveals clear and rapid convergence as $i_{\max}$ increases. This is expected, as larger $i_{\max}$ values reduce the Crank-Nicolson time discretisation error, which is $O(\Delta t^2)$. A point of diminishing returns is reached around $i_{\max} = 2000$, which is adopted as a practical choice balancing accuracy and computational efficiency. The final parameters used to estimate the option value are therefore $j_{\max} = 20{,}000$, $i_{\max} = 2000$, and $r_{\max} = 4$.

With the parameters outlined in Sections 1.1 and 2.1, the best estimate of the option value, using $j_{\max} = 20{,}000$, $i_{\max} = 2000$, $r_{\max} = 4.0$, the option's value:

$$V(r_0, t = 0; T_1, T) = 2.833713081352163. \tag{36}$$